Photo-Ionization of Lithium: A Many-Body Calculation

Edward S. Chang* and M. R. C. McDowell*†
Laboratory for Theoretical Studies, Goddard Space Flight Center, National Aeronautics and Space Administration, Greenbelt, Maryland
(Received 21 June 1968)

The photo-ionization cross section a_ν of lithium has been calculated to second order in Brueckner-Goldstone perturbation theory with Hartree-Fock as zero order, for ejected electron energies in the range $0 \leq k^2 \leq 0.36$ Ry. Other Hartree-Fock calculations of a_ν are analyzed using certain new theorems relating alternative forms of the matrix element. The final second-order perturbed values of a_ν in the length and velocity formulations are in good agreement with experiment throughout the energy range studied.

I. INTRODUCTION

Recent experimental work[1,2] appears to have established accurate values for the photo-ionization cross section of atomic lithium from threshold to quite short wavelengths. The theoretical position is not so satisfactory. The most elaborate published calculation[3] is in poor agreement with experiment, while simpler Hartree-Fock calculations,[4,5] one of which (in one formulation) is in close agreement with experiment, disagree among themselves.

In this paper, we present some calculations of the photo-ionization cross section using a Brueckner-Goldstone many-body approach[6] with the Hartree-Fock model as the zero-order approximation. The theory is outlined in Sec. II. We re-investigate the Hartree-Fock model in Sec. III, obtaining certain new theorems which enable us to analyze the previous calculations[4,5] and clarify the relationship between the standard length, velocity, and acceleration formulations. In Sec. IV we investigate the effects of certain short-range correlations in initial and final states. Long-range (polarization) correlations are considered in Sec. V, and a pseudopotential method developed for evaluating these. Finally, in Sec. VI we compare our results with other calculations and with experiment.

II. THEORY

The photo-ionization cross section at frequency ν for an atomic system is given by[7]

$$a_\nu = (2\pi e^2\hbar^2/m^2c_\nu)\int d\Omega \left|\sum_j \int d\tau_N \times \Psi_f^*(N)\exp(i\vec{k}_\nu\cdot\vec{r}_j)\vec{p}_j\,\Psi_i(N)\right|^2,$$

where $\vec{p}_j$ is the momentum of the jth electron, and $\vec{k}_\nu$ is the momentum of the photon. The other symbols have their usual meaning. In the visible light region $\vec{k}_\nu\cdot\vec{r}$ is of the order 10^{-3} over the dimensions of the atom, and $\exp(i\vec{k}_\nu\cdot\vec{r})$ can be replaced by unity. Taking the values of the various constants from Bethe and Salpeter,[7]

$$a_\nu = 8.56\times10^{-19} S/(I+k^2)\omega \text{ cm}^2, \quad (1)$$

where $h\nu = I + k^2$, I is the ionization potential of the system, and k^2 is the energy of the ejected electron, in rydbergs. From this point on, we shall take $\hbar = c = a_0 = 1$, $m = \frac{1}{2}$, and $e^2 = 2$. Here ω is the statistical weight of the initial atomic state, and S is given by

$$S = 4\sum\left|\int \Psi_f^*(N)\nabla_N\Psi_i(N)\right|^2,$$

where $\nabla_N = \sum_{j=1}^{N}\nabla_j$,

the sum being over initial and final states. Here $\Psi_i(N)$ and $\Psi_f(N)$ are N-electron wave functions of such initial and final states, respectively, and $\nabla_j = ip_j$.

For alkali atoms in their ground $^2S_{1/2}$ state

$$S/\omega = 4|\sigma_V|^2, \quad \sigma_V = \int \Psi_f^*(N)\,\nabla_N\Psi_i(N)\,d\tau_N, \quad (2)$$

and σ_V is the N-electron velocity form of the matrix element.

This matrix element may be put in alternate forms by application of the N-electron commutator relation

$$[H, \vec{r}_N] = -\nabla_N, \quad (3)$$

where $\Psi_f(N)$ and $\Psi_i(N)$ satisfy

$$H\Psi_f(N) = E_f\Psi_f(N), \quad H\Psi_i(N) = E_i\Psi_i(N). \quad (4)$$

Thus the well-known N-electron "length" matrix element is given by

$$\sigma_L(N) = \int \Psi_f(N)\vec{r}_N\Psi_i(N)\,d\tau_N = [2/(E_i - E_f)]\sigma_V(N), \quad (5)$$

where $E_i - E_f = -(I + k^2)$ Ry, provided (4) is satisfied exactly. Hence

$$S/\omega = (I+k^2)^2|\sigma_L|^2. \quad (6)$$

Since $\Psi_i(N)$ and $\Psi_f(N)$ are not known exactly, they must be approximated in some way. In this

paper, we choose to make a perturbation theory expansion of these functions in terms of a zero-order Hamiltonian which corresponds to the fixed-core Hartree-Fock (H. F.) model (cf. Sec. III below). The perturbation theory is chosen so that the normalization of Ψ_i is preserved to the first order. The normalization factor $\langle\Psi_i \mid \Psi_i\rangle$ has been previously calculated[6] to be 1.0028 and is taken as unity in the present calculation. The requirement on Ψ_f is that

$$\int \Psi_f{}^*(k)\,\Psi_f(k')\,d\tau_N = \delta(k^2-k'^2);$$

i.e., that $\Psi_f(k)$ represents unit outgoing flux and is further discussed below. Furthermore since the photon operator has odd parity, Ψ_i and Ψ_f are of opposite parity, and necessarily orthogonal.

The application of the Brueckner-Goldstone technique to the ground of lithium $\Psi_i(N)$ has been described in detail elsewhere,[6] and it may readily be extended to the final state $\Psi_f(N)$. In this work, we express σ_L or σ_V as a sum of diagrams where the wiggly line represents the photon operator (in the appropriate formulation) acting between the one-electron states. These states, defined in Sec. III below, are members of a complete set of Hartree-Fock bound and continuum states. In the initial unperturbed state Φ_0 (the "vacuum" state), only the lowest three one-electron states ($1s\,\alpha$, $1s\,\beta$, $2s\,\alpha$) are occupied. These are called unexcited states, and all others are called excited states. Following previous workers, we define a "hole" as an unoccupied unexcited state shown in the diagrams by a downward-directed solid line, and a "particle" as an occupied excited state is indicated by an upward directed solid line (cf. Fig. 1). As usual the interelectron interaction $r_{ij}{}^{-1}$ is represented by a horizontal dotted line and the Hartree-Fock potential V_{HF} is indicated by a horizontal dotted line ending in a cross (cf. Fig. 3).

For example, the zero-order diagram [1(a)] corresponds to the fixed-core Hartree-Fock approximation

$$\sigma^{\mathrm{HF}} = \langle\Phi_k|\vec{O}|\Phi_0\rangle, \tag{7}$$

where the photon operator $\vec{O}$ is given by ∇_N in the velocity formulation (2) and by $\vec{r}_N$ in the length formulation (6), and Φ_k is the final unperturbed state. The $|\Phi_k\rangle$, $|\Phi_0\rangle$ are constructed (as single Slater determinants) from one-electron fixed-core Hartree-Fock orbitals ϕ_t, defined in Sec. III below. In general these two approximations,

$$S_L{}^{\mathrm{HF}} = \omega(I+k^2)^2\,|\sigma_L{}^{\mathrm{HF}}|^2 \tag{8a}$$

and

$$S_V{}^{\mathrm{HF}} = 4\omega|\sigma_V{}^{\mathrm{HF}}|^2, \tag{8b}$$

are not equivalent.

The initial and final states correspond to the configurations $|1s,1s,2s\rangle$ and $|1s,1s,kp\rangle$, respectively. The first-order initial state diagrams [1(b) and 1(c)] correspond to certain correlations in $\Psi_i(N)$ involving the configurations $|1s,np,kp\rangle$, $|1s,k'p,kp\rangle$ [Fig. 1(b)] or $|1s,kp,np\rangle$, $|1s,kp,k'p\rangle$ [Fig. 1(c)]. The dominant contributions come from $k' \gg k$, and therefore may be interpreted as a short-range correlation effect. Similar effects arise in the final state and are represented by Figs. 1(d) and 1(e). They correspond to the configurations $|1s,k'p,2s\rangle$ and $|1s,2s,k'p\rangle$. In each case the notation $k'l$ for the intermediate excited states implies a summation over bound l states ($k'^2 < 0$) and an integration over the continuum. In practice we sum over the lowest eight bound l states and use an n^{-3} rule[6] to estimate the contribution from the remainder. In all the first-order diagrams evaluated in this paper, the bound intermediate state contribution ($n \leq 8$) was less than 10% of the total and the contribution from $n > 8$ was negligible.

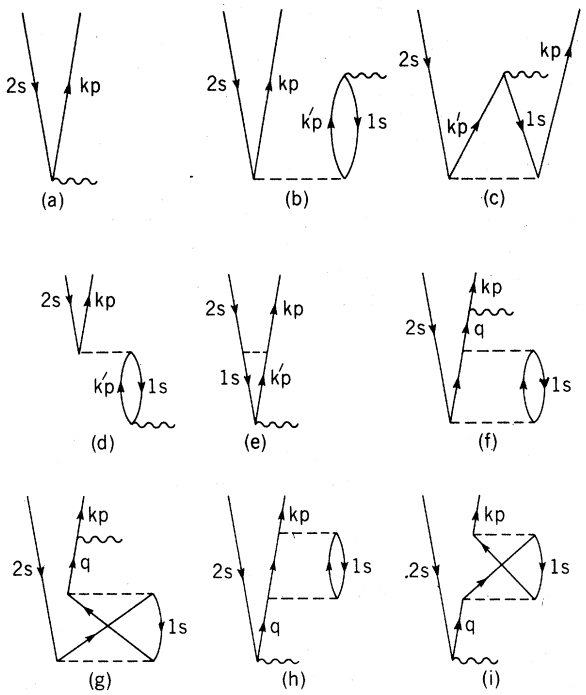

FIG. 1. Diagrams corresponding to zero-, first-, and second-order contribution to the initial and final wave functions. The states are labeled as in the text. A ~~~ means a photon operator and a dashed horizontal line represents v.

There are many second-order diagrams. We show only those which give the dominant contribution to the ($1s^2$) core polarization [Figs. 1(f)–1(i)], and represent long-range correlations. The second-order diagrams corresponding to short-range correlations have been discussed elsewhere,[6] and may be neglected in comparison with Figs. 1(b)-1(e), as may contributions to S arising from transitions between the short-range correlation parts of Ψ_i and Ψ_f. The second-order corrections to Φ_0 which we consider are those given by Figs. 1(f) and 1(g). They correspond to configurations $|1s,1s,k'l \pm 1\rangle_{l=1}$ or

$|1s,k'l \pm 1,1s\rangle\ l=1$, respectively. The final-state second-order corrections [Figs. 1(h) and 1(i)] correspond to configurations $|1s,1s,np\rangle$, $|1s,np,1s\rangle$ (where n runs over all bound and continuum orbitals).

Rules for evaluating the contribution from a given diagram may be found in previous papers.[6] Examples will be given in Secs. IV and V. For now it suffices to say that a diagram specifies the appropriate matrix elements and energy denominators involved, with an over-all sign to be determined by $(-1)^{h+l+N}$, where h is the number of internal hole lines, l the number of closed loops, and N the number of times V_{HF} appears in the diagram. Note that the energy denominators are given by subtracting the energy of the perturbed state from the unperturbed state. In the initial state (below the photon line), the energy of the unperturbed state is $2\epsilon_{1s}+\epsilon_{2s}$, but in the final state (above the photon line), the energy of the unperturbed state is $2\epsilon_{1s}+k^2$.

In the next three sections we consider, in more detail, the contributions from each order in turn.

III. HARTREE-FOCK APPROXIMATION

For lithium-like systems, the restricted Hartree-Fock approximation takes a particularly simple form. In particular if $\phi_{1s}{}^{(0)}$ is the Hartree-Fock solution[8] for the $1s$ orbital (in the $1s^2 2s\ {}^2S_{1/2}$ configuration) then the one-electron Schrödinger equation

$$[h(i)-\epsilon_{nl}]\phi_{nl}(i)=0 \tag{9}$$

$$\text{with}\quad h(i)=-\nabla_i^2-(2Z/r_i)+2\langle\phi_{1s}{}^{(0)}(j)|(1/r_{ij})(2-P_{ij})|\phi_{1s}{}^{(0)}(j)\rangle, \tag{10}$$

where $P_{ij}f(i,j)=f(j,i)$. It has been shown[6] that $h(i)$ has a complete orthogonal set of solutions ϕ_t, which are the fixed core Hartree-Fock orbitals. Some authors[4,5] replace $\phi_{1s}{}^{(0)}$ by the corresponding $(1s^2\ {}^1S_0)$ Li^+ orbital. The differences are of order one percent, and are not significant in our work.

From Sec. II, the Hartree-Fock length (σ_L^{HF}) and velocity (σ_V^{HF}) matrix elements are given by Eqs. (8a) and (8b) above. The corresponding one-electron matrix elements are

$$\sigma_L^{\mathrm{HF}}=\sigma_{0,L}=\sqrt{3}\,\langle\phi_{kp}(i)|\vec{r}_i|\phi_{2s}(i)\rangle \tag{11a}$$

$$\text{and}\quad \sigma_V^{\mathrm{HF}}=\sigma_{0,V}=\sqrt{3}\langle\phi_{kp}(i)|\nabla_i|\phi_{2s}(i)\rangle. \tag{11b}$$

We now derive a theorem relating these. We note first that the one-electron Hamiltonian $h(i)$ does not satisfy the commutator relation (3). Rather, since

$$[-\nabla_i^2-(2Z/r_i),\vec{r}_i]=-2\nabla_i \tag{12}$$

$$\text{we have}\quad [h(i),\vec{r}_i]=-2\nabla_i+2[V_{\mathrm{HF}},\vec{r}_i], \tag{13}$$

$$\text{where}\quad V_{\mathrm{HF}}=\langle\phi_{1s}{}^{(0)}(j)|(1/r_{ij})(2-P_{ij})|\phi_{1s}{}^{(0)}(j)\rangle. \tag{14}$$

Now the direct term of V_{HF} does commute with $\vec{r}_i$, but the exchange term (involving P_{ij}) does not. Thus by Eq. (9)

$$\langle\phi_k(i)|[h(i),\vec{r}_i]|\phi_{2s}(i)\rangle=(k^2-\epsilon_{2s})\langle\phi_k(i)|\vec{r}_i|\phi_{2s}(i)\rangle=(k^2-\epsilon_{2s})\sigma_{0,L}, \tag{15}$$

but from (11) to (14)

$$\langle\phi_k(i)|[h(i),\vec{r}_i]|\phi_{2s}(i)\rangle=-2\sigma_{0,V}-2\langle\phi_k(i)|[\langle\phi_{1s}{}^{(0)}(j)r_{ij}^{-1}P_{ij}\phi_{1s}{}^{(0)}(j)\rangle,\vec{r}_i]|\phi_{2s}(i)\rangle. \tag{16}$$

We define radial functions by

$$\phi_{nl}(\vec{r})=(1/r)P_{nl}(r)Y_{lm}(\hat{r}),$$
$$\int_0^\infty P_{nl}(r)P_{n'l}(r)dr=\delta_{nn'}, \tag{17}$$
$$\int_0^\infty P_{kl}(r)P_{k'l}(r)dr=\delta(k^2-k'^2),$$

$$\text{so that}\quad P_{kl}(r)\sim k^{-1/2}\sin[\zeta(r)+\delta_l] \tag{18}$$

and $\xi(r)$ is defined by Burgess.[9,10] Then using (17) in (16) and integrating over angles

$$\int_0^\infty P_{kp}(r) r P_{2s}(r)dr = [2/(k^2-\epsilon_{2s})]\{\int_0^\infty P_{kp}(r)[1/r - d/dr]P_{2s}(r)dr + \tfrac{1}{3}I_1 - I_2\}, \tag{19}$$

where

$$\begin{aligned} I_1 &= \int_0^\infty dr_2 P_{1s}(r_2)P_{kp}(r_2)[(1/r_2^2)\int_0^{r_2} dr_1 P_{1s}(r_1)P_{2s}(r_1)r_1^2 + r_2\int_{r_2}^\infty dr_1 P_{1s}(r_1)(1/r_1)P_{2s}(r_1)], \\ I_2 &= \int_0^\infty dr_2 P_{1s}(r_2)P_{kp}(r_2)[(1/r_2)\int_0^{r_2} dr_1 P_{1s}(r_1)P_{2s}(r_1)r_1 + \int_{r_2}^\infty dr_1 P_{1s}(r_1)P_{2s}(r_1)]. \end{aligned} \tag{20}$$

That is $$\sigma_{0,L} = [2/(k^2-\epsilon_{2s})](\sigma_{0,V} + \tfrac{1}{3}I_1 - I_2) \tag{20'}$$

and by Koopmans' theorem[11] we may write this as

$$\sigma_{0,L} = [2/(I+k^2)](\sigma_{0,V} + \tfrac{1}{3}I_1 - I_2). \tag{21}$$

Similarly, since

$$[\nabla_i, h(i)] = \nabla_i(-2Z/r_i + 2V_{\mathrm{HF}}), \tag{22}$$

we have

$$(k^2-\epsilon_{2s})\int_0^\infty P_{kp}(r)(1/r - d/dr)P_{2s}(r)dr = 2[-Z\int_0^\infty P_{kp}(r)(1/r^2)P_{2s}(r)dr + 2I_3 - I_4 - I_5 + \tfrac{1}{3}I_6], \tag{23}$$

where

$$\begin{aligned} I_3 &= \int_0^\infty dr_2 P_{kp}(r_2)P_{2s}(r_2)(1/r_2^2)\int_0^{r_2} dr_1 P_{1s}^2(r_1), \\ I_4 &= \int_0^\infty dr_2 P_{kp}(r_2)P_{1s}(r_2)(1/r_2^2)\int_0^{r_2} dr_1 P_{1s}(r_1)P_{2s}(r_1), \\ I_5 &= \int_0^\infty dr_2 P_{kp}(r_2)[P_{1s}'(r_2) - P_{1s}(r_2)/r_2][(1/r_2)\int_0^{r_2} dr_1 P_{1s}(r_1)P_{2s}(r_1) + \int_{r_2}^\infty dr_1 P_{1s}(r_1)P_{2s}(r_1)/r_1], \\ I_6 &= \int_0^\infty dr_2 P_{kp}(r_2)P_{1s}(r_2)\{(1/r_2^2)\int_0^{r_2} dr_1 P_{1s}(r_1)[P_{2s}'(r_1) - P_{2s}(r_1)/r_1]r_1 \\ &\quad + r_2\int_{r_2}^\infty dr_1[P_{1s}(r_1)/r_1^2][P_{2s}(r_1) - P_{2s}'(r_1)/r_1]\}, \end{aligned}$$

and the prime on a function indicates its derivative. That is, defining the acceleration form of the Hartree-Fock one-electron matrix element as

$$\sigma_A^{\mathrm{HF}} = \sqrt{3}Z\langle \phi_{kp}(r)|\cos\theta/r^2|\phi_{2s}(r)\rangle = Z\int_0^\infty P_{kp}(r)(1/r^2)P_{2s}(r)dr, \tag{24}$$

we have the theorem

$$\sigma_V^{\mathrm{HF}} = [2/(I+k^2)][\sigma_A^{\mathrm{HF}} - 2I_3 + I_4 + I_5 - \tfrac{1}{3}I_6]. \tag{25}$$

These results may be extended readily to other atomic systems.

Stewart[4] and Sewell[5] have each reported fixed core Hartree-Fock calculations of a_ν for Li. Stewart and Sewell choose the 1s-ion core. Their results and ours are shown in Fig. 2. Our calculation of σ_V^{HF} gives identical results to Stewart's, but it is in marked disagreement with Sewell's work. Stewart's length result is not strictly Hartree-Fock, as he was forced to fit his tabulated[12] $P_{2S}(r)$ to a Bates-Damgaard function[13] at $r = 5a_0$, and it lies between his velocity result and our length result. Again we disagree markedly with Sewell's calculation of σ_L^{HF}.

Fortunately our first theorem [Eq. (20′)] enables us to test our calculations unambiguously. Our calculated values of σ_L^{HF} and σ_V^{HF} [defined by Eqs. (11a) and (11b), respectively] satisfy (20′) to one part in 10^4.

Stewart[4] gave results for a_ν in the acceleration formulation as well. His threshold values using σ_A^{HF} were a factor of approximately 20 high. He was aware of the possible existence of a result of the type given by our second theorem (25) but did not obtain it. We note that our calculated values of σ_A^{HF} agree with Stewart's, and are related to our calculated values of σ_V^{HF} by (25), again to an accuracy

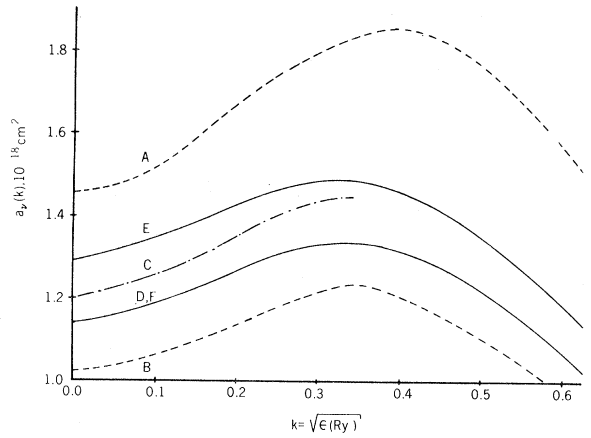

FIG. 2. Hartree-Fock calculations of the photoionization cross section of Li. A, Sewell (1967) length; B, Sewell (1967) velocity; C, Stewart (1954) length; D, Stewart (1954) velocity; E, this paper, length; F, this paper, velocity.

of 1 in 10^4. The resultant large value of a_v obtained using σ_A^{HF} arises because the gradient of the potential $-Z/r$ in (24) is essentially replaced by

$$Q(r_1) = (Z/r_1^2) - (2/r_1^2)\int_0^{r_1} P_{1s}^2(r_2)dr_2$$

in (25). At the small values of r_1 important in calculating a_v this potential is very nearly $1/r_1^2$, thus a_v is approximately a factor of Z^2 lower than the Hartree-Fock acceleration value.

In our formulation σ_V^{HF} is the fundamental form of the zero-order matrix element, and the corresponding results $a_v(\mathrm{HF}\,V)$ are in poor agreement with experiment, lying 25% below the most probable experimental values and outside reasonable (10% systematic, 10% random) error bars on these.[14]

We therefore consider higher-order effects in the next two sections.

IV. FIRST-ORDER CORRECTIONS

The diagrams corresponding to first-order correlation corrections to the ground state are shown in Figs. 1(b) and 1(c). A dashed horizontal line represents a correlation via the two-electron operator $v = 1/r_{12}$. The total Hamiltonian operator is

$$H = \sum_{i=1}^{3} h(i) + H' = \sum_{i=1}^{3} \left[-\nabla_i^2 - \frac{2Z}{r_i} + 2V_{\mathrm{HF}}(i)\right] + H' \tag{26}$$

$$\text{so that} \quad H' = 2\sum_{i>j}^{3} \frac{1}{r_{ij}} - 2\sum_{i=1}^{3} V_{\mathrm{HF}}(i). \tag{27}$$

However, V_{HF} does not appear in the perturbation diagrams because it is canceled by certain terms involving v. In diagrammatic notation,[6] the cancellation occurs as shown in Fig. 3 and is

$$\langle k_s | V_{\mathrm{HF}} | k_t \rangle = 2\langle k_s, 1s | v | k_t, 1s\rangle - \langle k_s, 1s | v | 1s, k_t\rangle . \tag{28}$$

The matrix element represented by Fig. 1(b) is

$$(1b) = 2(4/\pi)\int_0^\infty k_s dk_s \langle 1s | \vec{O} | k_s p\rangle \langle k_s p, kp | v | 1s, 2s\rangle / (\epsilon_{1s} + \epsilon_{2s} - k_s^2 - k^2). \tag{29}$$

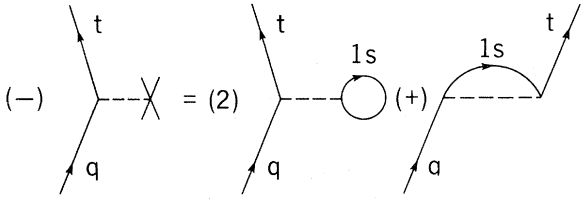

FIG. 3. Cancellation of the Hartree-Fock perturbation (- - -X) by certain other diagrams involving v, shown by only the appropriate sub-diagram.

Here, the external factor of 2 arises because there are two $(1s\alpha, 1s\beta)$ possible $1s$ "holes," while the over-all sign of the matrix element is positive, since in addition to the internal hole line, there is one closed loop. The energy denominator is found as the difference in energies of the perturbed and unperturbed states as $(E_0 - E')$ where $E_0 = 2\epsilon_{1s} + \epsilon_{2s}$, $E' = \epsilon_{1s} + \epsilon_{k_s} + \epsilon_{kp} = \epsilon_{1s} + k_s^2 + k^2$, so that $(E_0 - E') = \epsilon_{1s} + \epsilon_{2s} - k_s^2 - k^2$. The corresponding exchange diagram Fig. 1(c) has no closed loops, and only the $(1s\alpha)$ hole contributes; hence it gives

$$(1c) = -(4/\pi)\int_0^\infty k_s\, dk_s \langle 1s|\vec{O}|k_s p\rangle \langle kp, k_s p|v|1s, 2s\rangle / (\epsilon_{1s} + \epsilon_{2s} - k_s^2 - k^2). \tag{30}$$

Similarly, Figs. 1(d) and 1(e) give the direct and exchange first-order final-state correlation contributions, the energy denominator now being $(E_k - E') = (2\epsilon_{1s} + k^2) - (\epsilon_{1s} + k_s^2 + \epsilon_{2s})$; hence

$$(1d) = 2(4/\pi)\int k_s\, dk_s \langle k_s p|\vec{O}|1s\rangle \langle k_s, kp|v|k_s p, 2s\rangle / (\epsilon_{1s} - \epsilon_{2s} + k^2 - k_s^2) \tag{31}$$

and

$$(1e) = -(4/\pi)\int k_s\, dk_s \langle k_s p|\vec{O}|1s\rangle \langle 1s, kp|v|2s, k_s p\rangle / (\epsilon_{1s} - \epsilon_{2s} + k^2 - k_s^2). \tag{32}$$

The two-electron matrix elements had been previously calculated,[6] while the remaining matrix element is just the Hartree-Fock length or velocity matrix element from an initial $1s$ orbital. The integrands contain no singularities, and were evaluated by a Simpson's rule. The intermediate set of states denoted by $|k_s p\rangle$ includes all bound p states together with an integration $(2/\pi)\int k_s dk_s$ over continuum p states. The calculations were performed for both length and velocity operators, $\vec{O} = \vec{r}_N$ and ∇_N, respectively, and the results are shown in Table I. The corresponding first-order corrected length and velocity cross sections, together with the zero-order results and experiment, are shown in Fig. 4. The first-order velocity correction is appreciably larger than the first-order length correction so that the length and velocity results are now in better accord. However, they are still about 15% below the most probable experimental values.

In both length and velocity formulations the dominant contributions come from intermediate state momenta k_s in the range $1.0 < k_s < 2.0$ so they correspond to short-range correlation. In both cases this type of correlation is approximately twice as large in the final $1s^2 kp$ configuration as in the initial $1s^2 2s$ configuration. However, while in the length form both are additive with respect to the zero-order effect, in the velocity formulation the initial-state first-order contribution is of opposite sign to the zero-order matrix element.

V. SECOND-ORDER CORRECTIONS

The dominant second-order correction is due to the polarization of the $1s^2$ Li^+ core. Consider the direct diagrams labeled 1(f) and 1(h). The sub-diagram shown in Fig. 5 represents the dominant contribution to the polarization.[15] It yields a contribution of 0.174 to the theoretical polarizability of 0.19 (Lahiri and Mukherjee[16]) which is in good agreement with the measured value.[17] We note that singularities will occur in the integrand for some second-order diagrams for Ψ_f. For example, Fig. 1(h) contains an energy denominator $(\epsilon_{kp} - \epsilon_q)$ which vanishes when $k_q^2 = k^2$. In principle,

TABLE I. Calculated contributions to the lithium photo-ionization matrix element, σ_L or σ_V as functions of ejected electron momentum k. L indicates length formulation and the V velocity formulation, while the first subscript indicates the order of perturbation theory considered, and a second subscript (i or f) indicates whether in initial or final state. L_{tot} and V_{tot} are our final results.

k (Ry$^{1/2}$)	L_0	L_{1i}	L_{1f}	L_{2i}	L_{2f}	L_{tot}	V_0	V_{1i}	V_{1f}	V_{2i}	V_{2f}	V_{tot}
0.05	1.963	0.0138	0.0232	−0.041	0.279	2.232	−0.3670	+0.0476	−0.0714	+0.0027	−0.0450	−0.4331
0.10	1.966	0.0136	0.0231	−0.040	0.266	2.229	−0.3749	+0.0478	−0.0757	+0.0026	−0.0441	−0.4403
0.15	1.965	0.0133	0.0228	−0.037	0.250	2.214	−0.3870	+0.0482	−0.0723	+0.0025	−0.0427	−0.4513
0.20	1.955	0.0129	0.0226	−0.034	0.233	2.190	−0.4019	+0.0486	−0.0729	+0.0021	−0.0410	−0.4651
0.25	1.931	0.0124	0.0222	−0.030	0.211	2.156	−0.4183	+0.0490	−0.0735	+0.0018	−0.0389	−0.4799
0.30	1.889	0.0118	0.0217	−0.026	0.190	2.087	−0.4347	+0.0498	−0.0747	+0.0014	−0.0368	−0.4950
0.35	1.830	0.0112	0.0212	−0.022	0.165	2.005	−0.4500	+0.0504	−0.0756	+0.0010	−0.0340	−0.5082
0.40	1.754	0.0105	0.0206	−0.018	0.146	1.913	−0.4631	+0.0512	−0.0768	+0.0006	−0.0319	−0.5200
0.45	1.665	0.0095	0.0200	−0.014	0.125	1.806	−0.4738	+0.0518	−0.0777	+0.0001	−0.0289	−0.5285
0.50	1.567	0.0090	0.0194	−0.011	0.108	1.692	−0.4816	+0.0526	−0.0789	−0.0003	−0.0268	−0.5350
0.55	1.464	0.0083	0.0187	−0.008	0.093	1.576	−0.4866	+0.0534	−0.0801	−0.0006	−0.0244	−0.5383
0.60	1.358	0.0075	0.0181	−0.005	0.078	1.457	−0.4888	+0.0542	−0.0813	−0.0010	−0.0242	−0.5411

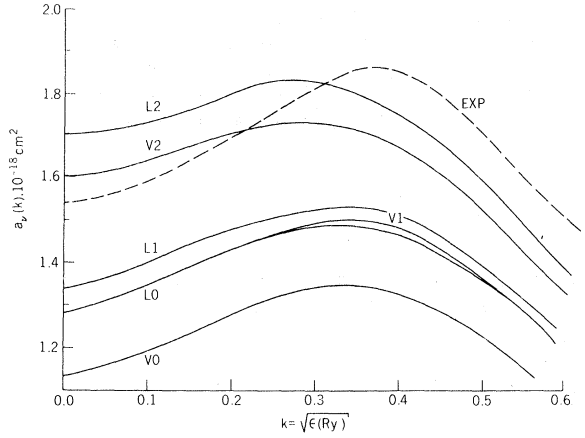

FIG. 4. Corrections to the Hartree-Fock calculations of the photo-ionization cross section of Li; $L0$, $L1$, and $L2$ are length formulation with zero-, first-, and second-order contributions included, respectively, $V0$, $V1$, and $V2$ are the corresponding velocity results, and the dashed curve (EXP) shows the quoted experimental results of Hudson and Carter (1967).

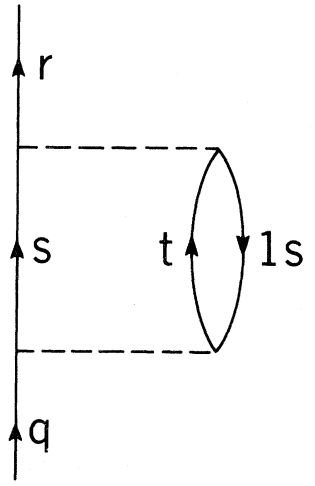

FIG. 5. Core polarization sub-diagram involving a single core excitation.

it is possible to evaluate the integral by a principal value technique, but the loss of numerical accuracy is not easy to assess. We now show that the contribution of these diagrams to the photo-ionization matrix element may instead be calculated by a pseudopotential technique. The potential contains all multipole contributions, and its direct part corresponds to 1(f) [or 1(h)] while it has an exchange-polarization part corresponding to 1(g) [or 1(i)]. Several authors have shown[15,18,19] that the calculated solutions are but little affected if only the dipole term of the direct polarization potential is retained, all other multipoles and exchange polarization being neglected. We have confirmed this in detail in one case, discussed in the Appendix.

Consider diagram 1(f). Its contribution to the photo-ionization matrix element is

$$\langle 1f\rangle = 4(2/\pi)^3 \int k_s dk_s \langle kp|\vec{O}|k_s s\rangle$$

$$\times \int k_1 dk_1 \int k_2 dk_2 \frac{\langle 1s,k_s s|v|k_1 l_1,k_2 l_2\rangle\langle k_1 l_1,k_2 l_2|v|1s,2s\rangle}{(\epsilon_{1s}+\epsilon_{2s}-k_1^2-k_2^2)(\epsilon_{2s}-k_s^2)}. \tag{33}$$

The second matrix element is sharply peaked at $k_2=k_S$. We replace k_2 by k_S in the denominator (which in any case is dominated over the range of k_2 of importance by ϵ_{1S}) and can then perform the closure over $|k_2 l_2\rangle$ states. (The procedure is given in detail for part of Fig. 1(h) in the Appendix.) The result may be written as

$$(1f) = 4\left(\frac{2}{\pi}\right)^2 \int k_s dk_s \langle kp|\vec{O}|k_s s\rangle \int k_t dk_t \frac{\langle k_s s|J_t^2|2s\rangle}{(\epsilon_{1s}+\epsilon_{2s}-k_t^2-k_s^2)(\epsilon_{2s}-k_s^2)}. \tag{34}$$

Now define a pseudopotential

$$\mathcal{V} = (4/\pi)\int k_t dk_t \frac{J_t^2}{(\epsilon_{1s}+\epsilon_{2s}-k_t^2-k_s^2)}, \quad J_t(1) = \langle 1s(2)|(1/r_{12})|t(2)\rangle \tag{35}$$

and consider the perturbation by it. The relevant Schrödinger equation is

$$[h(i)+\mathcal{V}+\bar{\epsilon}_{2s}]\,\chi(\vec{r}) = 0, \tag{36}$$

where $\bar{\epsilon}_{2s}$ is the required eigenvalue. This may be put in integral equation form

$$\chi(\vec{r}_1) = |2s,\vec{r}_1\rangle + \int d\vec{r}_2 G(\vec{r}_1,\vec{r}_2,\bar{\epsilon}_{2s})\mathcal{V}(\vec{r}_2)\chi(\vec{r}_2),$$

$$G(\vec{r}_1,\vec{r}_2,\bar{\epsilon}_{2s}) = 2\sum_t{}' |t\rangle\langle t|/(\bar{\epsilon}_{2s} - \epsilon_t), \tag{37}$$

and to first order in v the iterated solution is formally

$$\chi(\vec{r}_1) = |2s,\vec{r}_1\rangle + \int d\vec{r}_2 G(\vec{r}_1,\vec{r}_2,\epsilon_{2s})v(\vec{r}_2)|2s,\vec{r}_2\rangle. \tag{38}$$

Thus the additional contribution to the matrix element is

$$\begin{aligned}(1f) &= \langle kp|\vec{O}|\chi\rangle - \langle kp|\vec{O}|2s\rangle = \langle kp|\vec{O}[\int dr_2 G(\vec{r}_1,\vec{r}_2,\bar{\epsilon}_{2s})v(\vec{r}_2)|2s,\vec{r}_2\rangle]\rangle \\ &= (4/\pi)\int k_s dk_s[\langle kp|\vec{O}|k_s s\rangle(\bar{\epsilon}_{2s} - \epsilon_s)]\langle k_s|v|2s\rangle \end{aligned} \tag{39}$$

which is Eq. (34). Second-order final diagrams [for example, Fig. 1(h)] which involve singular energy denominators are evaluated by the same technique, except that (36) is now a scattering equation for an electron in the field of the polarized ion core. Note that the pseudopotential technique ensures that Ψ_f is correctly normalized to unit flux. In practice we approximate v by an adiabatic potential

$$V_{ad} = (4/\pi)\int k_t dk_t \mathcal{I}_t/(\epsilon_{1s} - k_t^2).$$

The potential V_{ad} is asymptotic to $-\alpha_0/r^4$ with $\alpha_0 = 0.174$, but it cannot be expressed in closed analytic form. It differs little (cf. Appendix) from the Bethe potential[19–21] (with $\kappa = z_1 r, z_1^4 = 9/\alpha_0$),

$$V_{pol}^{(1)}(\kappa) = (9/\kappa^4)[1 - \tfrac{1}{3}(1 + 2\kappa + \kappa^2 + 6\tfrac{2}{3}\kappa^3 + \tfrac{4}{5}\kappa^4)e^{-2\kappa} - (1+\kappa)^4 e^{-4\kappa}], \tag{40}$$

which is the dipole component of

$$V_{pol} = 2\left\langle \bar{1}s|v|\sum_{\bar{q}\neq 1s}\frac{\langle\bar{q}|v|\bar{1}s\rangle}{\epsilon_{1s}^{(0)} - \epsilon_q^{(0)}}\bar{q}\right\rangle = \frac{4}{\pi}\int k_t dk_t \frac{\bar{\mathcal{I}}_t^2}{\epsilon_{1s}^{(0)} - \epsilon_t^{(0)}}, \quad \bar{\mathcal{I}}_t = \langle\bar{1}s|v|\bar{t}\rangle. \tag{41}$$

Here the states $|\bar{t}\rangle$ are a complete set of hydrogenic states with nuclear charge $Z_1 = (9/\alpha_0)^{1/4}$ chosen to describe two hydrogenic electrons with the diagram polarizability α_0, and having eigenvalues $\epsilon_t^{(0)}$.

Our calculations were therefore performed with $V_{pol}(\vec{r})$ rather than with $v(\vec{r})$. A similar treatment applies to the final-state second-order correlation diagrams 1(h) and 1(i), except that rather than solving an eigenvalue equation for $\bar{\epsilon}_{2s}$, a scattering equation must be solved for the $l = 1$ phase shift. These have been reported elsewhere[22] and are in good agreement near threshold with the corresponding quantum-defect values.[23]

The resultant polarized 2s orbital is a little different from the Hartree-Fock 2s orbital, and consequently the second-order initial-state corrections are small (L_{2i} and V_{2i} of Table I) and in general of opposite sign to the zero-order matrix element. The effects on the free-electron function are larger, the p-wave phase shift at threshold increasing from 0.110 to 0.164 (whereas the quantum-defect value is 0.188). The correction to both length and velocity matrix elements is additive and about 10% of the zero-order matrix element. The over-all effect is to flatten the shape of the calculated cross section near threshold and increase its slope for energies higher than that at which the maximum occurs. The agreement with experiment (for both length and velocity) is satisfactory.

The contribution of third- and higher-order diagrams may be estimated by noting that each high order involves an additional factor of a matrix element ($\sim 10^{-1}$) divided by an energy denominator ($\sim\frac{1}{2}\epsilon_{1s} = 2.48$).

The contribution from an nth-order diagram ($n > 2$) is therefore estimated to be approximately 10% of that of the $(n-1)$ order diagram. Second-order final state is a special case, since it is the lowest order in which a vanishing energy denominator occurs. Higher-order diagrams involving one or more vanishing energy denominators can be reduced to modifications of 1(h) or 1(i), and since we have not approximated the solution of (37) by (38), but solved (36), they are to some extent included implicitly in that solution.

VI. CONCLUSIONS

Our final results (L_{tot} and V_{tot} of Table I) give length and velocity value for the cross section in better agreement with each other than the zero-order values, but less good than the first-order corrected values. A uniform convergence of the length to the velocity results with increasing order of approximation is not to be expected since it is known that if the exchange terms are omitted in zero order, the two results are then identical. However, the difference between our final length and velocity results is only half of the uncertainty of the experimental values, and any reasonable average of our two results differs (in the range of the calculation $0 \leq k \leq 0.6$) from the mean experimental result by less than 10%.

Tait (in 1964) has calculated the cross section in the length and the velocity formulations using a Hylleraas-type ground-state wave function, and a final-state wave function consisting of a Slater-type

core and a Hartree-Fock continuum orbital. His ground-state function includes primarily short-range correlation effects, which we have seen are small. However, his final-state function is so inadequate that it almost certainly is responsible for his poor results (Fig. 6), his length and velocity values differing by 60%.

We believe our final answers to be reliable to + 10%. The most important additional corrections would be the other contributing second-order diagrams which are of short-range type,[16] and are estimated to provide a 10% correction to (L_0-L_1) and (V_0-V_1); and, secondly, higher-order polarization diagrams which correct the polarizability of the Li^+ core from 0.174 to 0.19. Our method of evaluating polarization diagrams is equivalent to an adiabatic approximation in electron scattering. Nonadiabatic effects[15,18] could change our second-order correction by about 10%, as could the inclusion of intermediate $|k_S d\rangle$ states [in the notation of Eq. (33)] in these diagrams. The $\langle kp|\vec{O}|k_S d\rangle$ free-free matrix elements for the isoelectronic system He^- are less than 10% of the $\langle kp|\vec{O}|k_S s\rangle$,[24] and have consequently been neglected in our calculations for Li. The contribution to the matrix element from first-order correlation in both initial and final states simultaneously has been neglected because of the large energy denominators involved.

Thus our final values lie within the 10% random error of the experimental numbers throughout the energy range considered.

APPENDIX. REDUCTION OF THE SECOND-ORDER SUMS

We consider in detail those contributions from diagrams 1(h) and 1(i) in which the photon first raises the $2s$ electron into a polarized $2p$ orbital in order to justify our use of V_{ad} in Sec. 5. The relevant diagrams are given in Figs. 1(h) and 1(i), where the state q is specifically the $2p$ state.

Now consider the direct diagram 1(h). For each $1s$ hole this gives

$$(1h)=\frac{16}{\pi^2}\langle 2p|\vec{O}|2s\rangle \int k_s dk_s \int k_t dk_t \frac{\langle 1s,kp|v|k_t l_t,k_s l_s\rangle\langle k_t l_t,k_s l_s|v|1s,2p\rangle}{(k^2-\epsilon_{2p})(\epsilon_{1s}+k^2-k_s{}^2-k_t{}^2)}, \tag{A1}$$

where the integrals over complete sets at this stage imply sums over intermediate angular momenta (l_s,m_{ls}) and (l_t,m_{lt}). These sums may be written as

$$C=\sum_{l_s m_{ls},l_t m_{lt}}\langle 1s,kp|v|k_t l_t,k_s l_s\rangle\langle k_t l_t,k_s l_s|v|1s,2p\rangle. \tag{A2}$$

Now expanding

$$v=1/r_{12}=\sum_{\lambda\mu}[4\pi/(2\lambda+1)]\gamma_\lambda(12)Y_{\lambda\mu}(\hat{r}_1)Y_{\lambda\mu}{}^*(\hat{r}_2), \tag{A3}$$

we have (in the notation of Edmonds[25])

$$C=\sum_{ls\lambda\mu}\frac{3(2l_s+1)}{(2\lambda+1)}\begin{pmatrix}1 & l_s & \lambda\\ 0 & 0 & 0\end{pmatrix}^2\begin{pmatrix}1 & l_s & \lambda\\ 0 & -\mu & \mu\end{pmatrix}^2 T_{l_s\lambda} \tag{A4}$$

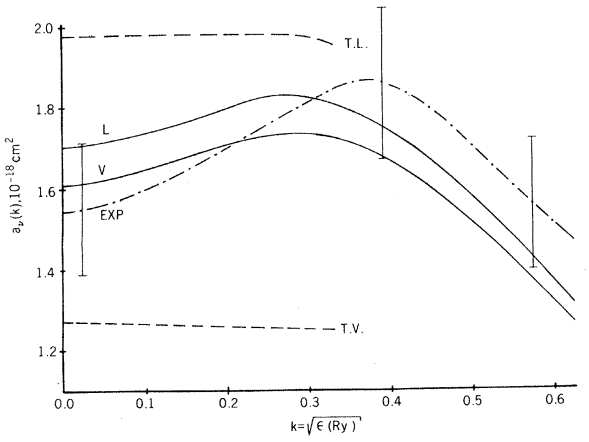

FIG. 6. Photo-ionization cross section of Li. T. L., T. V., Tait (1964) length and velocity; L, V, this paper, length and velocity; EXP, experiment of Hudson and Carter.

where $$T_{l_s\lambda} = \int_0^\infty \int_0^\infty P_{1s}(1)P_{2p}(2)\gamma_\lambda(12)P_{k_t l_t}(1)P_{k_s l_s}(2)dr_1 dr_2$$

$$\times \int_0^\infty \int_0^0 P_{1s}(3)P_{2p}(4)\gamma_\lambda(34)P_{k_t l_t}(3)P_{k_s l_s}(4)dr_3 dr_4. \tag{A5}$$

Now by definition of the Hartree-Fock states

$$(2/\pi)\int k_s dk_s P_{k_s l_s}(2)P_{k_s l_s}(4) = \delta(r_2 - r_4). \tag{A6}$$

Using this closure and replacing k_s by k in the denominator, (1h) becomes

$$(1h) = (8/\pi)\langle 2p|\vec{O}|2s\rangle \int k_t dk_t \sum_\lambda C_\lambda T_\lambda(k_t)/[(k^2 - \epsilon_{2p})(\epsilon_{1s} - k_t^2)] \tag{A7}$$

and $$C_\lambda = \sum_{l_s,\mu} \frac{3(2l_s+1)}{(2\lambda+1)} \begin{pmatrix} 1 & l_s & \lambda \\ 0 & 0 & 0 \end{pmatrix}^2 \begin{pmatrix} 1 & l_s & \lambda \\ 0 & -\mu & \mu \end{pmatrix}^2,$$

$$T_\lambda(k_t) = \int_0^\infty P_{kp}(r)P_{2p}(r)I_{\lambda,k_t}{}^2(r)dr \tag{A8}$$

with $$I_{\lambda,k_t}(r) = \int P_{1s}(r')\gamma_\lambda(r,r')P_{k_t\lambda}(r')dr'.$$

Evaluating the 3-j coefficients,

$$C_0 = 1, \quad C_1 = \tfrac{1}{3}, \quad C_2 = \tfrac{2}{25}, \ldots . \tag{A9}$$

Thus we can write (dropping a k_t subscript on the I_{λ,k_t} integrals)

$$2\times(1h) = \frac{8}{\pi}\langle 2p|\vec{O}|2s\rangle \int k_t dk_t \frac{\int_0^\infty 2(I_0{}^2 + \frac{1}{3}I_1{}^2 + \frac{2}{25}I_2{}^2 \cdots)P_{kp}(r)P_{2p}(r)dr}{(k^2 - \epsilon_{2p})(\epsilon_{2s} - k_t{}^2).} \tag{A10}$$

In using closure to reduce Eq. (A4) we have included the occupied 1s and 2s states, which now must be consistently subtracted out. The radial integral in (A10) requires to be reduced by

$$\tfrac{1}{9}[2\int_0^\infty P_{2p}P_{1s}I_1 dr' \int_0^\infty P_{kp}P_{1s}I_1 dr + \int_0^\infty P_{2p}P_{2s}I_1 dr' \int_0^\infty P_{kp}P_{2s}I_1 dr]. \tag{A11}$$

A similar analysis may be carried out for the exchange diagram (1i). The result for (1i) may be expressed in the form (A10) except that the radial integral is now

$$\tfrac{1}{3}\int_0^\infty P_{1s}(r)P_{kp}(r)(I_0J_1 + J_1I_0 + \tfrac{2}{5}I_1J_2 + \tfrac{2}{5}I_2J_1 + \cdots)dr, \tag{A12}$$

where $$J_\lambda(r') = \int_0^\infty P_{2p}(r')\gamma_\lambda(r,r')P_{k_t\lambda}(r')dr' \tag{A13}$$

and the appropriate subtraction is

$$\frac{1}{3}\sum_{n=1}^{2} \int_0^\infty P_{1s}(r)P_{ns}(r)J_0(r)dr \int_0^\infty P_{ns}(r')P_{kp}(r')I_1(r')dr'. \tag{A14}$$

The initial state second-order correlation may be handled similarly. We tabulate the results below (Table II) for the final-state contribution. It is clear that the sum of the direct monopole and quadrapole contributions is effectively canceled by the total exchange contribution as in the case for helium.[15] Consequently $V_{ad}(\vec{r})$ is closely equivalent to $V_{pol}{}^{(1)}(\vec{r})$.

TABLE II. The $2p$ contribution to the second-order final-state correction in the length formulation, as a function of ejected electron momentum k.

k ($Ry^{1/2}$)	0.2	0.4	0.6
$\lambda=0$, direct	0.0142	0.0100	0.0068
$\lambda=1$, direct	0.1417	0.0990	0.0647
$\lambda=2$, direct	0.0102	0.0073	0.0049
Eq. (A.10)	0.1661	0.1163	0.0764
Direct subtraction	0.0252	0.0177	0.0117
(A.10)−(A.11) = (a)	0.1409	0.0986	0.0647
Total exchange			
(A12)−(A14) = (b)	+0.0305	0.0221	0.0153
Total = (a) − (b)	0.1104	0.0765	0.0494

*National Academy of Sciences-National Research Council Post-Doctoral Resident Research Associates.
†On leave of absence 1967-1968 from University of Durham, England.

[1]R. D. Hudson and V. I. Carter, Phys. Rev. 137, A1648 (1965).
[2]R. D. Hudson and V. I. Carter, J. Opt. Soc. Am. 57, 651 (1967).
[3]J. H. Tait, Atomic Collision Process, edited by M. R. C. McDowell (North-Holland Publishing Co., Amsterdam, 1964), p. 586.
[4]A. L. Stewart, Proc. Phys. Soc. (London) 67, 917 (1954).
[5]K. G. Sewell, J. Opt. Soc. Am. 57, 1058 (1967).
[6]E. S. Chang, R. T. Pu, and T. P. Das, Phys. Rev. 174, 1, 16 (1968); K. A. Brueckner, Phys. Rev. 100, 36 (1955); J. Goldstone, Proc. Phys. Soc. (London) A239, 267 (1957); H. P. Kelly, Phys. Rev. 136, B896 (1964).
[7]H. A. Bethe and E. E. Salpeter, Quantum Mechanics of One and Two Electron Atoms (Academic Press, Inc., New York, 1957), pp. 299 *ff*.
[8]C. C. J. Roothaan, L. M. Sachs, and A. W. Weiss, Rev. Mod. Phys. 32, 186 (1960).
[9]B. Strömgren and M. Rudkjobing, Publ. Kbn. Obs. 18, 1 (1941).
[10]A. Burgess, Proc. Phys. Soc. 81, 442 (1963).
[11]T. Koopmans, Physica 1, 104 (1933).
[12]V. Fock and M. J. Petrashen, Physik. Z. Sowjetunion 8, 547 (1935).
[13]D. R. Bates and A. Damgaard, Phil. Trans. Roy. Soc. (London) A242, 101 (1949).
[14]We are indebted to Dr. Hudson and Dr. Carter for a discussion of their random and systematic errors.
[15]R. T. Pu and E. S. Chang, Phys. Rev. 151, 31 (1966).
[16]J. Lahiri and A. Mukherji, J. Phys. Soc. (Japan) 21, 1128 (1966).
[17]K. Bockaston, Arkiv Fysik 10, 867 (1956).
[18]R. W. LaBahn and J. Callaway, Phys. Rev. 135, A1339 (1964), and 147, 28 (1966).
[19]J. H. Williamson and M. R. C. McDowell, Proc. Phys. Soc. 85, 719 (1964).
[20]H. A. Bethe, Handbuch der Physik (Edward Brothers, Ann Arbor, Michigan, 1943), Vol. 24, Pt. 1, pp. 339 *ff*.
[21]J. Callaway, Phys. Rev. 106, 868 (1957). Our potential V_{ad} is much closer to that given by Eq. (19) of Callaway's paper than that given by his Eq. (17).
[22]M. R. C. McDowell, Phys. Rev. 175, 189 (1968).
[23]A. Burgess and M. J. Seaton, Monthly Notices Roy. Astron. Soc. 120, 121 (1960).
[24]M. R. C. McDowell, V. P. Myerscough, and J. H. Williamson, Astrophys. J. 144, 82 (1966).
[25]A. R. Edmonds, Angular Momentum in Quantum Mechanics (Princeton University Press, Princeton, New Jersey, 1957), pp. 46 *ff*.